ReLoc: Hybrid RSSI- and Phase-based Relative UHF-RFID Tag Localization with COTS Devices

Chenglong Li, Emmeric Tanghe, *Member, IEEE,* David Plets, *Member, IEEE,*
Pieter Suanet, Jeroen Hoebeke, Eli De Poorter, and Wout Joseph, *Senior Member, IEEE*

***Abstract*—Radio frequency identification (RFID) technology brings tremendous advancements in Industrial Internet-of-Things (IIoT), especially for smart inventory management, as it provides a fast, and low-cost way of counting or positioning items in warehouse. In the last decade, many novel solutions including absolute and relative positioning methods, have been proposed for this application. However, the available methods are quite sensitive to the minor changes in the deployment scenario, including the orientation of the tag and antenna, the materials contained inside the carton, tag distortion, multipath propagation, etc. To this end, we propose a hybrid relative passive RFID localization method (ReLoc) based on both the received signal strength indicator (RSSI) and measured phases, which orders the RFID tags horizontally and vertically. In this paper, phase-based variant maximum likelihood estimation is proposed for lateral positioning, and the RSSI profiles of two tilted antennas are compared with each other for level distinguishing. We implement the proposed positioning system ReLoc with commercial off-the-shelf RFID devices. The experiment in a warehouse shows that ReLoc is a powerful solution for practical item-level inventory management. The experimental results show that ReLoc achieves an average lateral and level ordering accuracy of 94.6% and 94.3%, respectively. Notably, when considering liquid or metal materials inside the carton, or tag distortion, ReLoc still performs excellently with more than 93% ordering accuracy both horizontally and vertically, indicating the robustness of the proposed method.**

***Index Terms*—Radio frequency identification (RFID), ultra high frequency (UHF), received signal strength indicator (RSSI), phase, multipath propagation, indoor localization, industrial Internet-of-Things (IIoT), inventory management, unmanned aerial vehicle (UAV).**

I. Introduction

SUPPLY chain businesses continue to increase in flexibility and complexity. The ever increasing success of e-commerce requires new supply chain solutions at every stage of operations, including continuous inventory management. Nowadays, most warehouse systems have adopted automatic identification technology such as barcodes or ultra high frequency radio frequency identification (UHF-RFID) tags for automated inventory control, since it helps to minimize the risk of manual errors [1], [2]. However, even though these automated methods are being used, inventory auditing is time-consuming and labor-intensive in warehouses, especially when stocks are bulky, and stored vertically. To overcome this, automated inventory management using unmanned vehicles [3]–[5], such as commercial unmanned aerial vehicles (UAV) or drones has gained interest both in academy and industry.

RFID technology has experienced a tremendous growth and development since its humble beginnings back in the 1940s. The remarkable technical advances in passive RFID-based localization have resulted in enhanced performance in fast, accurate, and convenient inventory management. The received signal strength indicator (RSSI)-based positioning methods have been proposed in [6], [7] for the low complexity and flexibility in hardware deployment. Unfortunately, RSSI is easily affected by the propagation environment, absorption and scattering, and antenna effects including impedance mismatch and polarization mismatch. To this end, some naive phase-based passive RFID positioning methods in time, frequency and space domain have been proposed in [8] for a fine-grained localization. Stemming from the concept of synthetic aperture radar (SAR), [9]–[11] proposed to utilize phase-based virtual synthetic aperture through a mobile RFID reader (or antenna) to improve the positioning resolution. In [4], the authors exploited a drone-mounted RFID reader to locate the tags on the ground using the SAR-based match function proposed in [11], which required Global Navigation Satellite System (GNSS) to provide the trajectory of drone. Based on a hyperbolic positioning method, [12], [13] discussed the possibility of anchor-free phase-based positioning for RFID tags for static applications, in which the constraint of less than half wavelength between the adjacent antennas was utilized to mitigate phase ambiguity. [14] proposed an indoor RFID positioning method through establishing the virtual stations, which estimated the angle of arrival (AoA) and distance according to the phase difference of arrival (PDoA) recorded by the RFID antenna array. Furthermore, there are also some novel works that realize quite good RFID positioning performance based on the machine learning framework [15], [16].

Meanwhile, there are extensive applications, such as logistic, inventory management in warehouse and library, favoring the relative order instead of obtaining the absolute position (SAR, hyperbolic method, etc.). In [17], OTrack proposed to distinguish the order of luggage on the conveyor based on the response reception ratio (RRR) of RSSI, when the target approaching to the given reading window. Rather than RSSI, a RFID ordering method STPP was proposed in [18] based on the spatial and temporal phase profile of measured phases.

Manuscript received xx, 2019; revised xx, 2020. This work is supported in part by the Excellence of Science (EOS) project MUlti-SErvice WIreless NETworks (MUSE-WINET), and IMEC co-financed project InWareDrones.

C. Li, E. Tanghe, D. Plets, and W. Joseph are with the WAVES group, Department of Information Technology, Ghent University-IMEC, 9052 Ghent, Belgium (e-mail: chenglong.li@ugent.be).

P. Suanet is with Aucxis cvba, 9190 Stekene, Belgium.

J. Hoebeke and E. De Poorter are with the IDLab group, Department of Information Technology, Ghent University-IMEC, 9052 Ghent, Belgium.

Through detecting the sequence and quantity of the phase profile's V-zone, STPP can realize horizontal and vertical order with relatively high accuracy. Based on the probability-based weighted SAR method, MobiTagbot [19] also achieved quite good relative positioning performance. To mitigate the impact of multipath effect, MobiTagbot dwelt at each sampling position for a while to collect the phases of all channels. In [20], HMO relative localization system was established based on the RSSI and phase changes. However, HMO was designed for the scenarios, where people are moving between the reader antennas and tags. The system may not be able to be applied for asset management directly, in case no object moves across the antennas and tags. In [21], RePos was proposed for relative localization based on the inter-tag range and angle estimations. Information entropy of the measured phases was constructed to distinguish the contaminated samples, which helped to improve the robustness of positioning performance under dynamic scenarios.

Despite extensive methods having been proposed for passive UHF-RFID tag localization during the last ten years, the practical applications still face challenging problems requiring further investigation, especially for the RFID-based automated inventory management in warehouses. We hypothesize that the available absolute or relative positioning methods presented in literature do not solve all of the listed challenges below, which will be analyzed in detail in Section II.

- **Orientation of tag and antenna**: According to our experiments, when rotating the tag or antenna (also reported in [22]), RSSI and measured phases deviate from the expected values, which may be not negligible for practical applications.
- **Material inside the carton**: No available positioning method considers different materials inside the parcels or boxes according to the authors' best knowledge, such as metal, liquid, plastic, glass, etc. Different materials inside the labeled object may affect the measured phases and RSSI.
- **Tag distortion**: During a practical deployment or transportation, the tags may easily be bent or folded. The distorted tag will also change the measured results on the basis of our experimental results.
- **Multipath propagation**: Multipath propagation exists indoor, especially in warehouses [23]. Although some literature claim their methods' effectiveness over fading channels, they are not flexible for commercial applications due to the deployment of a complicated hardware system [24] or discontinuous movement [19].

In this paper, we will solve the above challenges for practical applications in a warehouse, and propose a hybrid RSSI and phase-based positioning method (ReLoc) to obtain the horizontal and vertical order based on commercial off-the-shelf (COTS) devices. The main contributions of this paper are: (i) We present a comprehensive investigation of challenges for practical applications, including hardware diversity, orientation, material inside the carton, tag distortion, and multipath effect. Most of these have not been reported or solved before according to the authors' best knowledge. (ii) We propose a new lateral order algorithm based on the variant maximum likelihood estimation (MLE). The likelihood function is reconstructed based on *sine* trigonometric transformation, which solves the problem of tag diversity, phase ambiguity, and phase jumps, and improves the lateral resolution. (iii) RSSI profile-based method is proposed to distinguish different rack levels vertically. So the drones-mounted or robot-mounted RFID positioning system does not need to scan each rack level. It saves more time and power consumption (battery). (iv) Through comparing the RSSI profiles of two tilted antennas (upwards and downwards), we can distinguish the specific level without worrying about the impact of orientation, different materials, tag distortion, multipath propagation, etc. Furthermore, our method is based on COTS devices, and does not add any burden on changing the reader's or tag's hardware configuration.

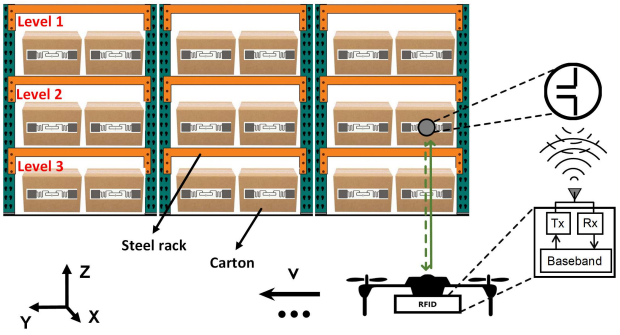

Fig. 1. Conceptual diagram of drone-based RFID positioning system for automated inventory management (Passive RFID tags are attached on the cartons, which are placed on the three-layers steel racks).

The remainder of this paper is organized as follows. Section-II presents the challenges of RFID tag positioning in warehouses, and analyzes the impacts of the system settings. In Section III, the relative RFID positioning system (ReLoc) is described, and the deployments of system hardware are discussed. The detailed algorithm of hybrid RSSI and phase-based level and lateral ordering is also presented in this section. In Section V, the setup of ReLoc positioning system is established, and the performance of proposed algorithm is evaluated and compared with state-of-the-art methods. Finally, Section V concludes this paper.

II. Challenges in Practical Applications

The communication between an UHF-RFID reader and a tag depends on the backscatter modulation as a result of the varying load impedance. For the RFID-based automated inventory management, especially in large-sized warehouses with high racks, a promising inventory method is mounting the RFID reader on a commercial unmanned robot or drones, as shown in Fig. 1. The robot (drone)-mounted reader moves along the racks with a given trajectory [10], [11], [13], or an unknown trajectory, which can be obtained using other vision-based or inertial sensors [2], [4], [5]. The on-board RFID reader localizes the tags stuck on the cartons based on the collected measurement data. Besides, as the racks can be stacked quite high (up to 16 meters), the on-board reader

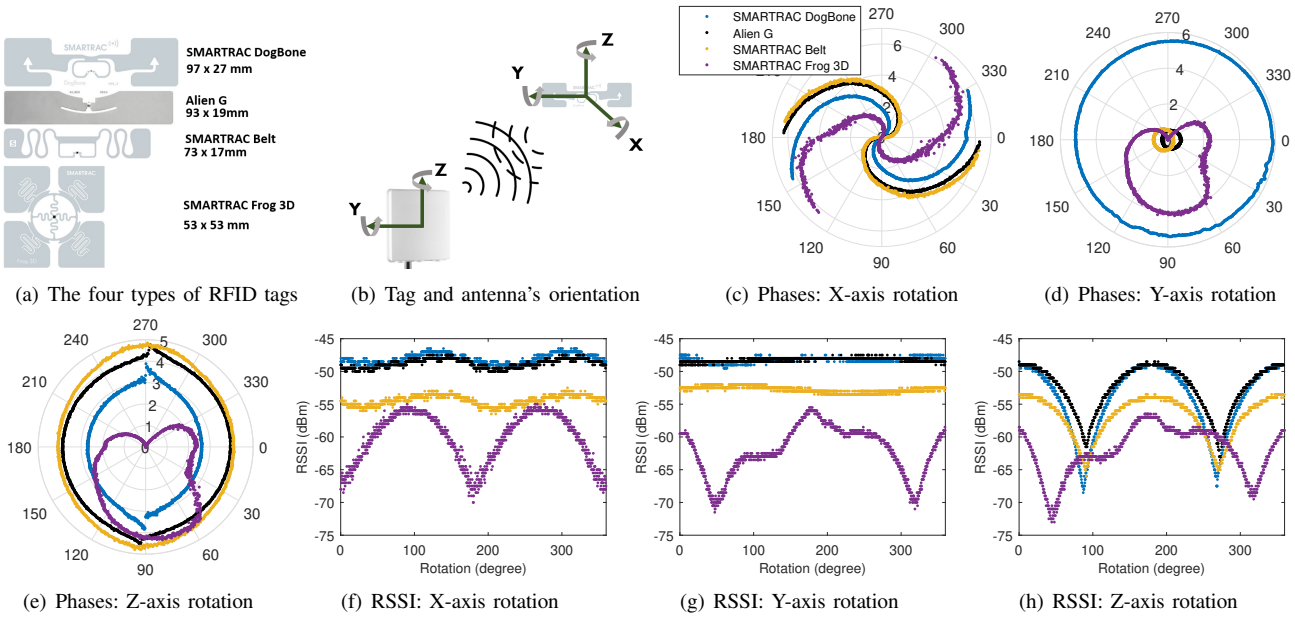

(a) The four types of RFID tags (b) Tag and antenna's orientation (c) Phases: X-axis rotation (d) Phases: Y-axis rotation

(e) Phases: Z-axis rotation (f) RSSI: X-axis rotation (g) RSSI: Y-axis rotation (h) RSSI: Z-axis rotation

Fig. 2. The configuration of orientation experiments using COTS RFID antenna Keonn Advantenna-SP11 and four types of COTS passive tags, and the impact of **tag orientations**: (c)-(e) measured phases (the angular axis is the tag rotation in degree and the radial axis is the measured phase in radian), (f)-(h) measured RSSI.

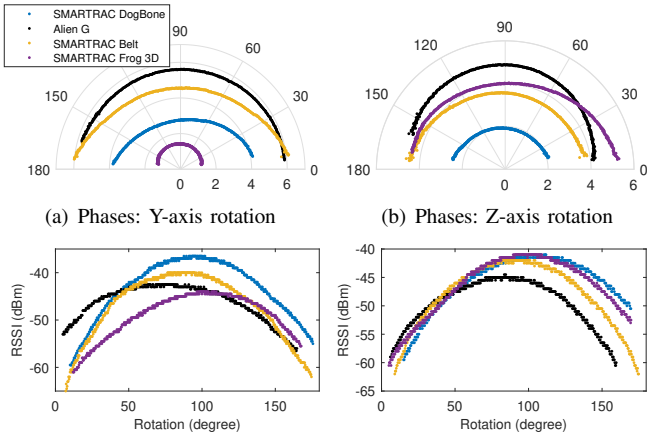

(a) Phases: Y-axis rotation (b) Phases: Z-axis rotation

(c) RSSI: Y-axis rotation (d) RSSI: Z-axis rotation

Fig. 3. The impact of **antenna orientations**: (a)-(b) measured phases (the angular axis is the tag rotation in degree and the radial axis is the measured phase in radian), (c)-(d) measured RSSI.

can avoid the accidents happening from manual inventory tracking, by scanning at two or more altitudes. Generally, the commercial RFID reader [25] can provide the low level user data: signal strength, phase and Doppler shift. Among them, the phase has been widely adopted for the potential fine-grained localization and sensing applications [4], [9]–[13], [19], [26]. One common point of these solutions is that they are all dependent on the precise positions of the antenna (reader), which can be provided by lidar, ultrasonic sensor, GNSS (outdoor scenarios) etc. However, the RFID positioning or sensing system is not used widely in commercial applications for automated inventory management yet. According to our experiments, we believe that from the perspectives of techniques, the reason is that the available RFID positioning systems are severely affected by minor changes of positioning scenarios, such as orientation of tag and antenna, materials contained inside the carton, tag distortion, multipath propagation, etc., which have not been solved perfectly yet. In this section, we will comprehensively investigate the impact of these factors on the RFID tag positioning.

A. *Orientation of Tag and Antenna*

In the orientation experiment, a COTS RFID reader Impinj Speedway R420, a Keonn Advantenna-SP11 UHF RFID antenna with 70-degree beamwidth, and four types of COTS passive tags: SMARTRAC DogBone, Alien G, SMARTRAC Belt, SMARTRAC Frog 3D are utilized to investigate the performance of the measured RSSI and phases, as shown in Fig. 2(a). In the experiment, the tags and antenna are mounted on a turntable in an anechoic chamber , which rotates continuously with a constant angular speed (12 degrees per second). As the sketch in Fig. 2(b) shows, the tags rotate 360 degrees in three dimensions, marked as X (roll), Y (pitch), and Z (yaw), while the antenna rotates 180 degrees in two dimensions (Y and Z). When rotating the tags or antenna, the geometry centers of the tags and the antenna are always aligned with each other. The initial positions of rotating tags are when their frontal sides are right facing with the antenna (in the plane of the Y-Z axes, as shown in Fig. 2(b)), while the initial position of rotating antenna is when the antenna is perpendicular to the tags. The distance from the antenna to the tags is about one meter. The transmitted power is set to 25 dBm, and the channel is 866.9 MHz [27].

1) Orientation of Tag: According to [26], the measured phase can be given by (1) as a result of modulo-2π operation,

$$\phi_m = \mathrm{mod}\Big(4\pi\frac{d}{\lambda} + \underbrace{\varphi_{Tx,Rx} + \varphi_{Tag}}_{:=\varphi_0}, 2\pi\Big), \tag{1}$$

where d represents the distance from the antenna to the tag, λ the wavelength, $\varphi_{Tx,Rx}$ the phase shift introduced by the transceiver's hardware circuit and wired cables, φ_{Tag} the phase shift caused by the tag. The measured phase is not only closely related with distance, but also the characteristic of the transceiver and RFID tag. When rotating the tag along the X-axis, we observe a full 2π-phase shifts in case of 180-degree rotation in Fig. 2(c). The measured phases are also different for the four tags even though the distance d is the same, which is called tag diversity. These two observations show that the phase shifts φ_0 caused by the tag cannot be calibrated easily due to the tag orientation in real-world deployment and tag diversity. Figs. 2(d)-(e) show that when rotating the tag along the Y-axis and Z-axis, the measured phases of the first three tags (SMARTRAC DogBone, Alien G, SMARTRAC Belt) have less than 0.12-radian fluctuations in case of $\pm$45-degree rotation at the point of 0 degree (initial position). The possible reasons for these minor errors are: (i) minor manual errors when conducting the experiments, (ii) the intrinsic hardware errors, such as not perfectly symmetric tag or antenna. A similar phenomenon has also been reported by [12], [22], [26]. But this is not the case for all types of RFID tags. For the SMARTRAC Frog 3D, the measured phases fluctuate distinctly with a maximum 1.8-radian shifts in case of $\pm$45-degree rotation at the point of initial position, which results from the inlay with two cross-linear antennas (see fig. 2(a)). For the phase-based positioning method, it is not possible to neglect such a large phase offset (1.8 radians), so the careful tag selection for specific application should be considered in practical applications.

For the monostatic backscatter link (with transceiver co-located), the RSSI in dBm can be given by [28]

$$RSSI = 10\log_{10}\left(\frac{P_t G_{Tx,Rx}^2 G_{Tag}^2 \lambda^4 X^2 M}{(4\pi d)^4 \Theta^2 B^2 F}\right), \qquad (2)$$

where P_t represents the transmitted power by the reader in watt, $G_{Tx,Rx}$, G_{Tag} are the gains of reader's antenna and tag, respectively, X is the polarization mismatch, M the modulation factor, Θ the tag's on-object gain penalty, B the path blockage loss, and F the monostatic fade margin. We can learn that the measured RSSI is also closely related with the environment and polarization mismatch. As shown in Fig. 2(f)-(h), when rotating the first three tags along the Y-axis, the RSSI values are almost constant. But for X-axis rotation, there are fluctuations up to 3 dB due to the polarization mismatch between the antenna and the tag, which has also been validated in [29], [30]. For the first three tags, they are based on a dipole antenna that is linearly polarized. But indeed, these tags are not pure dipoles, though their main polarization axis (Y-direction) seems to be horizontal. However, the tag antennas also have small vertical segments (Z-direction). Besides, depending on the design and even the manufacturer, the involved antenna may be more elliptically polarized than truly circularly. So when rotating the first three tags along the X-axis, there is polarization mismatch causing 2$\sim$3dB fluctuations. For the Z-axis rotation test, the RSSI fluctuates by about 5 dB offsets in case of $\pm$45-degree rotation at the point of initial position,

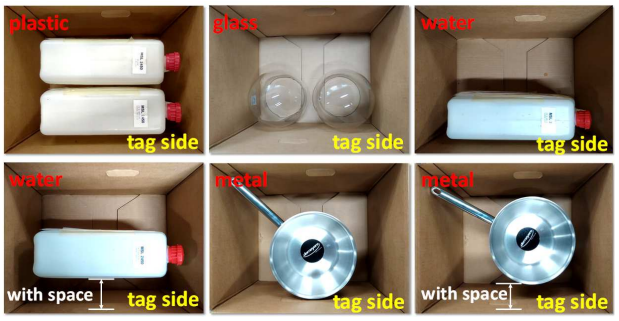

(a) The six cases of different materials placed inside the labeled box

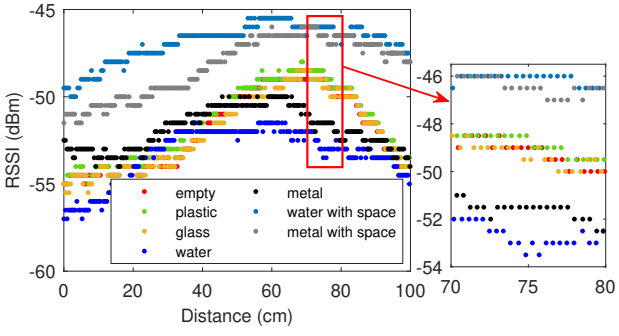

(b) RSSI

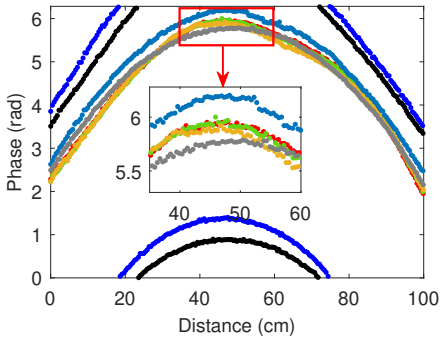

(c) Phases

Fig. 4. The performance of RSSI and phase in case of different materials.

which has not been considered for RSSI-based methods [6], [7]. For SMARTRAC Frog 3D, the observations are different from the other tags with more complex fluctuations. The phenomenon can be explained by the different radiation pattern (dual-dipole antenna) and polarization of SMARTRAC Frog 3D. Besides, they are not pure dipoles as mentioned above. We notice that the two perpendicular dipoles also have phase (frequency) offset due to the different length of the bending metal of the tag antenna. So when rotating the SMARTRAC Frog 3D tag, the RSSI exhibits even more fluctuations.

2) Orientation of Antenna: Rotating the antenna along X-axis can be regarded as the reverse operation of rotating the tag along X-axis. So when investigating the impact of antenna orientation, we only rotate the antenna (the radiation side) along Y/Z-axis with 180 degrees. The tag antenna gain can be regarded as a constant, since the tag is right in front of the tag and remains static. The changing parameter is the RFID antenna gain. As shown in Figs. 3(a)-(b), the measured phases are more stable when rotating the tag and antenna along Y/Z-

axis, which have about maximum 0.1-radian fluctuations in case of ±45-degree rotation at the point of 90 degree (initial position). Figs. 3(c)-(d) shows that RSSI shift about 3.5∼6 dB in case of ±45-degree rotation, which makes RSSI be an unreliable range-based metric.

When the antenna moves along the racks in warehouses, as shown in Fig. 1, it will not be possible to align the antenna with the tags (the case of Y/Z-axis tag and antenna rotation). Together with arbitrary tag deployment (X-axis tag rotation), there will be RSSI fluctuations due to antenna pattern and polarization mismatch as a result of the changing orientation.

B. Material Inside the Carton

Generally, we are aware of that the different materials where the tag attached will impact the measurements (both for RSSI and phase) [31]. But there is no literature reporting that the materials inside the parcels or boxes also affect the backscattered signal, and the positioning performance further. Fig. 4(a) shows the experimental setup. We investigate the impact by placing different materials into the tagged carton, namely plastic, glass, plastic tank filled with liquid (water), and metal. We set the measured results of the empty carton as the benchmark. The RFID antenna moves along the Y-axis as shown in Fig. 1, and the moving distance is one meter. The distance from the antenna to the rack is 1.2 meters, and the tag is placed at the midpoint (around 50 cm) of the linear trajectory. In Fig. 4, the Alien G RFID tag is selected. We also tested the other two types SMARTRAC DogBone and SMARTRAC Belt, which perform similarly as Alien G. The tag SMARTRAC Frog 3D is excluded here since it has been affected severely by the polarization mismatch as shown in Fig. 2(d)-(e),(g)-(h), when the antenna moves along the tag.

According to the measured results in Figs. 4(b)-(c), when placing plastic or glass inside the carton, both the RSSI and phases will have some minor shifts (less than 0.5 dB and 0.1 rad, respectively) compared with the case of empty box. Meanwhile, metal or liquid inside the box will not only correspondingly change the values of RSSI (up to 5 dB) and phase (1∼2 rad), but also the peaks' indexes of the measured RSSI slightly. It may due to the metal or liquid objects inside the carton changing the tag's radiation pattern. But when placing the metal or liquid object with a separation of about 10 centimeters to the tag, it only has slight impact on measured phases (less than 0.25-radian shifts), while it still affects the measured RSSI with up to 5-dB offsets. So we conclude that different materials (especially for metal and liquid) inside the tagged cartons will affect the performance of available RFID positioning systems.

C. Tag Distortion

In a practical deployment, the RFID tags' shape and surface may be distorted (bent or folded) because of the friction and collision during transfer or transportation, or even because the tagged objects themselves are with bent surface. In this paper, we also investigate the performance of the measured RSSI and phases in this case. Fig. 5(a) shows three possible cases of a distorted shape for the same scenario: flat tag without

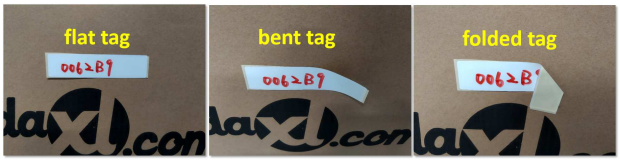

(a) The three possible cases of different shapes of tag

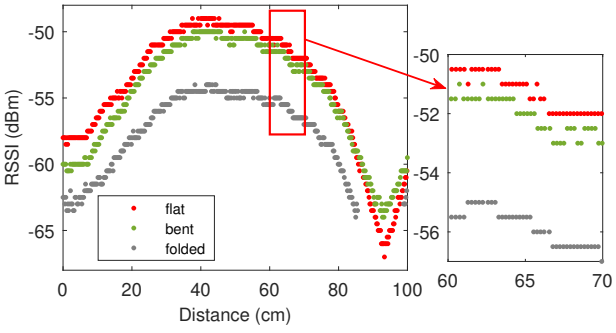

(b) RSSI

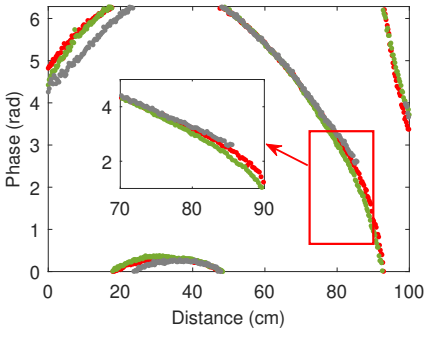

(c) Phases

Fig. 5. The performance of RSSI and phase with tag's different shapes.

distortion, bent tag with random numbers of degree and folded tag (part of the tag is folded). RFID tags with types Alien G, SMARTRAC DogBone and SMARTRAC Belt are selected for the measurements, while Fig. 5 only presents the experimental results of Alien G. Figs. 5(b)-(c) show the measured results for three cases of the distorted tag. The measured RSSI from the bent tag has small shifts (0.5∼2 dB) while the measured phase almost has no offset compared to the flat tag. As for the folded tag, the RSSI experiences about 5-dB shifts, which will degrade the performance and robustness of RSSI-based methods severely. We observe that folding the tag also causes the loss of recorded samples and minor shifts of the measured phases (less than 0.3 rad).

D. Multipath Propagation

Multipath propagation widely exists for indoor scenarios, especially in industrial warehouses with prevalent metal racks and a complex inventory deployment [23]. When conducting the RFID positioning in warehouses, the received signal not only includes the modulated signal backscattered from the tag, but also some reflected or scattered signal as a result of multipath propagation. As seen in Fig. 6, we investigate the RSSI and phase for four channels (namely, 865.7 MHz, 866.3 MHz,

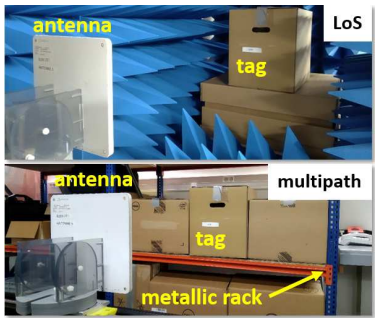

(a) Measurement scenarios

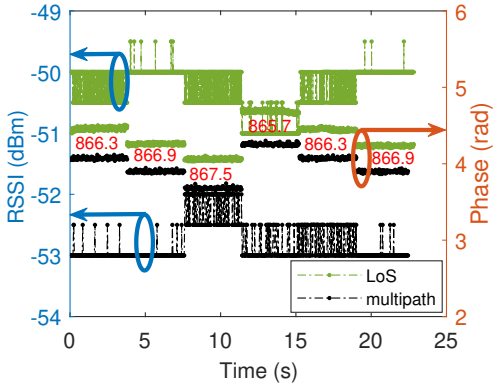

(b) Measured results

Fig. 6. The measured RSSI and phases with/without multipath.

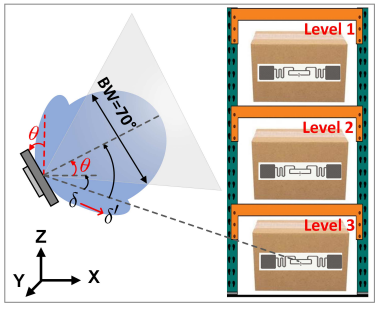

(a) Antenna rotation

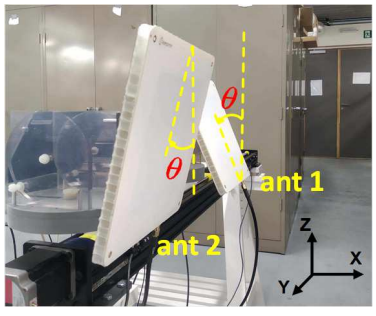

(b) Two tilted antennas

Fig. 7. Rotating antenna enables level discrimination.

866.9 MHz, and 867.5 MHz*). The distance from the tag to the antenna is 1.2 meter. For the multipath scenario, we conduct the experiment in a real indoor scenario, which mimic a small warehouse with some metallic racks and items, as shown in Fig.6 (a). The measured phases under multipath channel go through some stable shifts (about 0.4 rad) compared with the line-of-sight (LoS) channel. For the signal strength, the RSSI decreases about 2.5 dB in case of the multipath scenario, which results from the negative augmentation of channel fading. There is some literature claiming their effectiveness under multipath scenario, but they are mostly based on complex hardware deployments (discontinuous motion of the platform [19], software defined radio [24], large antennas array [14], [32], and computer vision [33]), which may be not adaptable to the commercial applications of the RFID positioning system in warehouses, such as the drone-mounted platform as shown in Fig. 1.

E. Brief Summary

Practical challenges for RFID positioning system design, related to tag and antenna orientation, material inside the carton, tag distortion and multipath propagation, are summarized below.

1) Orientation of Tag and Antenna: An X-axis tag rotation results in arbitrary measured phases, which means that the initial phase caused by the tag orientation cannot be calibrated in advance (before the phase-based positioning campaign). RSSI is sensitive to the orientation of the RFID tag (Z-axis rotation) and antenna (Y/Z-axis rotation). Therefore, RSSI is not a reliable metric for absolute positioning system. Furthermore, a careful tag selection (tag diversity) should be considered in the system design.

2) Material Inside the Carton: When placing specific materials inside the carton, especially liquid and metal (see Fig. 4), the measured RSSI and phase have significant offsets compared with the empty carton. In this case, both RSSI and phase become unreliable, making traditional RFID positioning methods not applicable.

3) Tag Distortion: According to the measurement results, tag distortion will also cause measurement offsets, especially for folded tags. This will also cause the loss of records, and has not been considered in available RFID positioning solutions.

4) Multipath Propagation: Multipath is one of the key factors in the degradation of the RFID positioning performance, causing fluctuations in the measured RSSI and phase. How to avoid its negative effect to the greatest extent should be taken into consideration in the positioning system design.

III. System Design

A. Heuristic Proposals

As illustrated in Section II, RSSI is sensitive to the orientation of the RFID tag and antenna due to polarization mismatch, different materials inside the tagged object, tag distortion, and multipath effects. Therefore, the RSSI is not a reliable indicator of precise absolute position estimation when the antenna moves along the tag. The measured phases are more reliable than RSSI, but also suffer from the different materials, and multipath effects to some extent. Fortunately,

*Another interesting finding is that channel hopping will produce constant shifts (about 0.24 rad per 0.6 MHz) while the RSSI do not show distinct frequency dependence on such a narrow frequency band.

although the above factors affect the value of measured phases, they almost do not change the peak index of phase when the antenna is right in front of the tag. So we still can use phase-based method for lateral localization. When the drone-based antenna moves linearly along the racks, as shown in Fig. 1, the phase-based method can localize the position of RFID tag in the direction of antenna's trajectory. We denote this as **lateral ordering**. This means that if we can find a method to distinguish different levels (the altitude in Fig. 1), we can obtain the relative order of the tags both horizontally and vertically.

As shown in Fig. 3(c), it is interesting to find that when rotating the antenna along the Y-axis with 45 degrees, RSSI shifts are about 3.5∼6 dB. Intuitively, the RSSI shifts caused by rotating the antenna can be used to realize the relative position discrimination. Inspired by the observation, a placement scheme of the RFID positioning system via antenna rotation has been proposed, as shown in Fig. 7(a). We rotate the antenna along Y-axis upwards (downwards) with θ as presented, making the incidence angle $\delta' = \delta + \theta$ of the tag of level three (one) is larger than half the beamwidth (35° for Keonn Advantenna-SP11). δ is the incidence angle in case of vertical-deployment antenna (no rotation), which is decided by the distance from the antenna to the rack. In this way, we also can identify these two levels based on the RSSI offsets resulting from antenna rotation, namely **level discrimination**. Normally, we can distinguish different levels based on the antenna rotation-based methods using only one antenna. However, only one antenna for relative positioning is not reliable because of the following reasons:

- Different materials are placed inside the tagged cartons or parcels: especially, when placing metal or liquid objects inside the carton as shown in Fig. 4, RSSI measured by a single antenna becomes unreliable.
- Not fully occupied racks: when some of the levels are empty, there may be no reference for RSSI comparison, since single antenna-based schemes need to compare the RSSI from each level to order the tags vertically.

To make the RFID positioning system self-consistent, we implement one more antenna. As shown in Fig. 7(b), we deploy two antennas tilted upwards and downwards with θ, respectively. We compare the RSSI profiles from the same tag of the two antennas, namely *differential* scheme. We denote the RSSI from the $i-$th antenna as $\mathrm{RSSI_i}$, $(i = 1, 2)$, so there are three cases due to the level distinguishing:

- **Level 1**: $\mathrm{RSSI_1} - \mathrm{RSSI_2} = \gamma_0 > 0$,
- **Level 2**: $\mathrm{RSSI_1} = \mathrm{RSSI_2}$,
- **Level 3**: $\mathrm{RSSI_1} - \mathrm{RSSI_2} = -\gamma_0 < 0$.

where γ_0 represents the RSSI difference caused by an antenna rotation over θ degrees. Different materials inside the carton and not fully occupied racks will not affect the level discrimination, since we only compare the RSSI differences of a single tag based on the above criterion. It should be noted that the criterion is too ideal for real-world applications. For practical deployments, the criterion should be modified as the one presented in Section III.C. Furthermore, we only consider three-level distinguishing in this paper. For the on-rack deployment in warehouses, the tags on level four or lower will easily be affected by record loss as a result of being far away from the main beam of the COTS antenna, especially when the antenna is tilted upwards. Furthermore, the measured phases will also be not reliable in this case due to the polarization mismatch (large-degree rotation). To manage multiple racks (more than three levels), we can just scan at one or more altitudes. From the perspective of algorithm design, the three-level distinguishing is practical and efficient for the on-rack positioning in warehouses. The drones-mounted or robot-mounted RFID positioning system does not need to scan each rack level, which saves more time and reduces power consumption (battery).

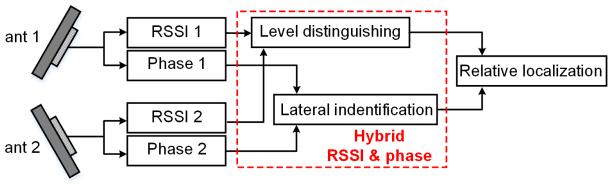

Fig. 8. Flow chart of hybrid RSSI and phase-based relative positioning system.

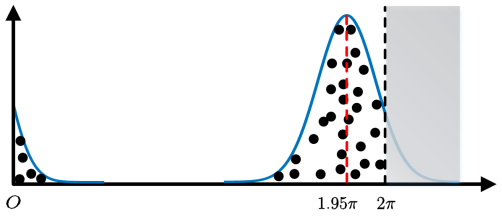

Fig. 9. An example of phase jump when actual phase is 1.95π.

We compare the RSSI profiles from the same tag of two tilted antennas. The two antennas have the same system settings, except for different rotation angles along Y-axis. Importantly, the two antennas will experience almost the same multipath propagation when moving along the RFID tag, if there is no change of the scenario settings. To this end, the impact of different materials, tag distortion, not full-rack deployment and multipath effect can be mitigated through the *differential* scheme since the only RSSI difference is caused by the rotation angle along Y-axis, which is used to distinguish different levels. The procedure of the proposed RFID relative positioning system (ReLoc) is shown in Fig. 8. Here, the RSSI from the two tilted antennas are used to distinguish the levels and the measured phases to identify the relative order laterally. The detailed algorithm description will be given in the following subsections.

B. Phase-based Lateral Positioning

As reported in [10], [12], [13], [19], [26], the measured phases of the RFID tag follow a Gaussian distribution $\phi_m \sim \mathcal{N}(\mu, \sigma^2)$, so we can use MLE to solve the positioning problem. Considering N independent observations of the measured

phases, the position of the targeted tag can be given as

$$\begin{aligned}\mathbf{P}_t &= \arg\max_{\mathbf{P}_t} \prod_{n=0}^{N-1} \frac{1}{\sqrt{2\pi}\sigma} e^{-\frac{\left(\phi_m[n]-\mathrm{mod}\left(\frac{4\pi}{\lambda}d[n]+\varphi_0\right)\right)^2}{2\sigma^2}} \\ &= \arg\max_{\mathbf{P}_t} \sum_{n=0}^{N-1}\left[-\left(\phi_m[n]-\mathrm{mod}\left(\frac{4\pi}{\lambda}d[n]+\varphi_0\right)\right)^2\right],\end{aligned} \tag{3}$$

where $\mathrm{mod}(\cdot)$ is the modulo-2π operator. $d = \|\mathbf{P}_a - \mathbf{P}_t\|$ is the distance from the position of antenna $\mathbf{P}_a = (x_a, y_a, z_a)$ to the position of tag $\mathbf{P}_t = (x_t, y_t, z_t)$. For a linear trajectory as shown in Fig. 1, $\mathbf{P}_a[n] = (x_a, y_a[n], z_a)$, where x_a and z_a are constant. $y_a[n]$ is related with the motion of the antenna. Since we only care about the lateral position of the tag, the problem in (3) can be written as

$$y_t = \arg\min_{y_t} \sum_{n=0}^{N-1}\left[\phi_m[n]-\mathrm{mod}\left(\frac{4\pi}{\lambda}\sqrt{(y_a[n]-y_t)^2+d_{xz}^2}+\varphi_0\right)\right]^2, \tag{4}$$

where $d_{xz}^2 = (x_a - x_t)^2 + (z_a - z_t)^2$. Due to the tag diversity, tag orientation (X-axis rolling in Fig. 2(c)) and frequency diversity [19], [34], the phase shift φ_0 varies and cannot been calibrated in advance. But for the given tag and antenna, φ_0 can be regarded as a constant even though there are small fluctuations due to polarization mismatch when the antenna is moving along the tag (equivalent to rotating the tag and the antenna along Y/Z-axis in Figs. 2(d)-(e) and Figs. 3(a)-(b)). To this end, a differential elimination is introduced to mitigate the impact of φ_0. It utilizes the phase differences between each sampling position $\phi_m[n]$ and the selected reference point $\phi_m[r]$, namely $\Delta\phi_m^{[n,r]} = \phi_m[n] - \phi_m[r]$. Define $\varphi_d^{[n]} = \mathrm{mod}\left(\frac{4\pi}{\lambda}\sqrt{(y_a[n]-y_t)^2+d_{xz}^2}+\varphi_0\right)$, then (4) is converted as

$$y_t = \arg\min_{y_t} \sum_{n=0}^{N-1}\left(\Delta\phi_m^{[n,r]} - \Delta\varphi_d^{[n,r]}\right)^2, \tag{5}$$

where $\Delta\varphi_d^{[n,r]} = \varphi_d^{[n]} - \varphi_d^{[r]} \in (-2\pi, 2\pi)$, so

$$\begin{aligned}\Delta\varphi_d^{[n,r]} &= \mathrm{mod}\left(\frac{4\pi}{\lambda}\sqrt{(y_a[n]-y_t)^2+d_0}+\varphi_0\right) \\ &\quad -\mathrm{mod}\left(\frac{4\pi}{\lambda}\sqrt{(y_a[r]-y_t)^2+d_0}+\varphi_0\right) \\ &= \begin{cases}\mathrm{mod}\left(\frac{4\pi}{\lambda}\Delta d^{[n,r]}\right)-2\pi, & \Delta\varphi_d^{[n,r]} \in (-2\pi, 0) \\ \mathrm{mod}\left(\frac{4\pi}{\lambda}\Delta d^{[n,r]}\right), & \Delta\varphi_d^{[n,r]} \in [0, 2\pi)\end{cases},\end{aligned} \tag{6}$$

where $\Delta d^{[n,r]} = \sqrt{(y_a[n]-y_t)^2+d_0} - \sqrt{(y_a[r]-y_t)^2+d_0}$. The phase uncertainty φ_0 is mitigated through the conversion in (6). However, the judging condition $\Delta\varphi_d^{[n,r]} \gtrless 0$ is an unknown prophet (chicken and egg problem), because the prerequisite of obtaining $\Delta\varphi_d^{[n,r]}$ is to judge the sign of itself.

Moreover, when the true phase is very close to 2π rad (or 0 rad), as shown in Fig. 9, the measured phases may jump to the value left to the 0 rad (or right to the 2π rad) as a result of the modulo-2π operation. So the likelihood function $f_{NLF}(\Delta\phi_m^{[n,r]}|d) = -\left(\Delta\phi_m^{[n,r]} - \Delta\varphi_d^{[n,r]}\right)^2$ in (5), say the naive likelihood function (NLF), will cause large errors as a result of $\Delta\phi_m^{[n,r]}$ abruptly jumping when the measured phases are around 2π or 0 rad. For example, when the actual phases are $\phi_m[r] = 1.6\pi$ rad and $\phi_m[n] = 1.95\pi$ rad, the phase difference $\Delta\phi_m^{[n,r]} = 0.35\pi$ rad. But due to the noise or other interference, $\phi_m[n]$ may jump to 0.03π rad, then $\Delta\phi_m^{[n,r]} = -1.57\pi$ rad, which brings a large offset to the NLF. To cope with the discontinuities caused by phase jumps, a trigonometric function transformation is introduced. The *sine* function is a good choice to realize this and makes the function values before and after phase jumps approaching to each other. We find that NLF in (5) has a good match with *sine* function utilizing the Taylor series approaching method, namely *sine* likelihood function (SLF), defined by $f_{SLF}(\Delta\phi_m|d)$. So the positioning estimation is given as

$$\begin{aligned}y_t &= \arg\min_{y_t} \sum_{n=0}^{N-1}\left(\Delta\phi_m^{[n,r]} - \Delta\varphi_d^{[n,r]}\right)^2 \\ &\doteq \arg\min_{y_t} \sum_{n=0}^{N-1} \underbrace{\sin\left(\Delta\phi_m^{[n,r]} - \Delta\varphi_d^{[n,r]}\right)^2}_{f_{SLF}(\Delta\phi_m^{[n,r]}|d)}.\end{aligned} \tag{7}$$

It should be noted that the trigonometric transformation in (7) also mitigates the condition judgment in (6), since the -2π compensation when $\Delta\varphi_d^{[n,r]} \in (-2\pi, 0)$ will not change the value of SLF as a result of *sine* transformation. Moreover, the *cosine* transformation in [26], and the periodic function $\exp\{j(\cdot)\}$ in SARFID [4], [11] can also solve the discontinuities caused by phase jumps. It can be explained that the periodic function $\exp\{j(\cdot)\}$ in SARFID is composed by two trigonometric functions based on the Euler's formula, namely $\exp\{j(\cdot)\} = \cos(\cdot) + j\sin(\cdot)$, which mitigates the impact of 2π-phase jumps.

When positioning in warehouses, the measured phases may suffer from environmental clutter, noise, and multipath interference. The measured result at each sampling position will have a different reliability. In this paper, a weighted likelihood function is proposed to augment the positioning performance, in which the component with smaller bias will be augmented with larger weight. The weighted MLE can be given as

$$y_t = \arg\min_{y_t} \sum_{n=0}^{N-1} w[n] f_{SLF}(\Delta\phi_m^{[n,r]}|d), \tag{8}$$

where $w[n] \in [0, 1]$. As presented above, $\phi_m \sim \mathcal{N}(\mu, \sigma^2)$, so $\Delta\phi_m^{[n,r]} \sim \mathcal{N}(0, 2\sigma^2)$. So we can construct the weights based on the probability density function (PDF) of $\Delta\phi_m^{[n,r]}$, namely $w[n] = \eta \cdot f_{PDF}(\Delta\phi_m^{[n,r]})$, where η is to normalize the weights, and $f_{PDF}(\Delta\phi_m^{[n,r]})$ is the PDF of $\Delta\phi_m^{[n,r]}$, given by

$$f_{PDF}(\Delta\phi_m^{[n,r]}) = \frac{1}{\sqrt{4\pi}\sigma} e^{\frac{f_{NLF}(\Delta\phi_m^{[n,r]}|d)}{4\sigma^2}}$$

Likewise, due to the phase jumps and the unknown prophet problem, the weights can also be converted through the *sine* transformation. So the normalized weights are given as $w[n] = e^{f_{SLF}(\Delta\phi_m^{[n,r]}|d)}$ after omitting $4\sigma^2$ which can be regarded as a constant for the short-range UHF RFID links [26].

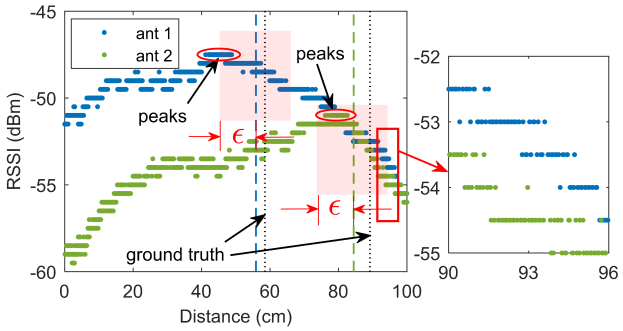

(a) RSSI

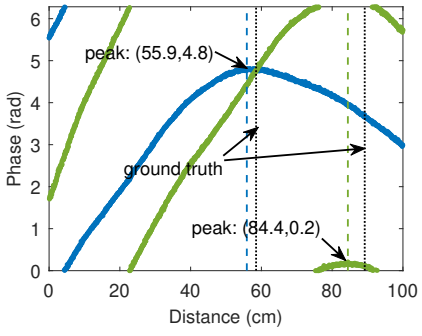

(b) Phases

Fig. 10. The profiles of RSSI and phases for two tilted antennas.

C. RSSI-based Level Distinguishing

As for passive RFID system, the RSSI decays as $1/d^4$ due to the round-trip free-space propagation between the antenna and tag. However, many factors can affect the RSSI, causing it to be different than predicted by the two-way radar equation: reflection and scattering, as well as the diversity of antenna and tag [8], [11], while the phase will be more reliable. Fig. 10 shows the profiles of RSSI and phase of the tag on level one when deploying the antennas as shown in Fig. 7(c). The profiles of RSSI go through distinct fluctuations due to the multipath effect and polarization mismatch. The black dot lines show the ground truth for the two antennas, while the blue and green dash lines show the peak indexes of the measured phases for the two antennas, respectively. The peak indexes of the RSSI profiles also have more than 10-centimeters shifts when the antenna moves along the tag. But for the phase profiles, they are more reliable with two definite peaks, which are due to the measured phases less easily affected by the polarization mismatch. It should be noted that the two antennas are mounted at the same altitude, and move along the tag one after the other. We can assume reasonably that the two antennas experience a very similar multipath environment, when the antennas move over the tag. In this way, the impact caused by multipath effect can be mitigated to a great extent.

To distinguish the tags on different levels, we can investigate the received RSSI from the two tilted antennas, namely $\mathrm{RSSI}_1 \underset{<}{\overset{>}{=}} \mathrm{RSSI}_2$. But due to the lateral polarization mismatch when the antennas move along the tags, the RSSI differences between two RSSI profiles should not be a constant as γ_0. Lateral polarization mismatch is the result of polarization mismatch when the antenna moves along the RFID tag laterally. It can be regarded as the case of both Y- and Z-axis rotation of the antenna or the tag in Section II.A, since the antenna and the tag may be not aligned with each other both laterally and vertically (not the same altitude) when the antenna moves along the tag. The intuitive method to solve this problem is to compare the RSSI without lateral polarization mismatch. To this end, we choose the neighborhood of RSSI profiles when the antennas are in front of the tag. Define the neighborhood as $\mathbb{U}_\epsilon = \{\mathrm{RSSI}(\ell) \big| |\ell - \ell_0^i| < \epsilon, i = 1, 2\}$, where ℓ_0 is the peak index when the antenna is right in front of the tag, which can be estimated by the phase-based lateral positioning method in Section III-B. ϵ represents half the length of the neighborhood $\mathbb{U}_\epsilon$. So the lateral polarization mismatch make no difference if we only compare the RSSI profiles within the defined neighborhood of the RSSI profiles. Besides, considering the measurement noise and the residual errors caused by channel fading and polarization mismatch, the judgment conditions can be modified as

- **Level 1**: $\mathrm{RSSI}_1^{\mathbb{U}_\epsilon} - \mathrm{RSSI}_2^{\mathbb{U}_\epsilon} > \gamma$,
- **Level 2**: $\mathrm{RSSI}_1^{\mathbb{U}_\epsilon} \approx \mathrm{RSSI}_2^{\mathbb{U}_\epsilon}$,
- **Level 3**: $\mathrm{RSSI}_1^{\mathbb{U}_\epsilon} - \mathrm{RSSI}_2^{\mathbb{U}_\epsilon} < \gamma$.

where γ is the given RSSI-offset threshold, when considering the residual errors mentioned above.

Notice that the number of recorded RSSI in the neighborhood $\mathbb{U}_\epsilon$ may vary due to the random access of RFID air interface protocol [27]. So we divide neighborhood $\mathbb{U}_\epsilon$ into K equal numbers of segments with the length $2\epsilon/K$, namely $\mathbb{U}_\epsilon = \{\mathbb{U}_\epsilon^1, \mathbb{U}_\epsilon^2, \cdots, \mathbb{U}_\epsilon^K\}$. Then we average the received RSSI in each segment, and define the following metric function

$$\varrho = \sum_{k=1}^{K} \left\lfloor \frac{\mathrm{RSSI}_1^{\mathbb{U}_\epsilon^k} - \mathrm{RSSI}_2^{\mathbb{U}_\epsilon^k}}{\gamma} \right\rfloor, \tag{9}$$

where $\mathrm{RSSI}_{\mathrm{i}}^{\mathbb{U}_\epsilon^k}$ is the mean RSSI at k-th segment of the i-th antenna. In case that the tag is on level one, $\mathrm{RSSI}_1^{\mathbb{U}_k} - \mathrm{RSSI}_2^{\mathbb{U}_\epsilon^k}$ will be larger than γ, so the metric ϱ will be close to K. Likewise, if the tag is on level three, ϱ will be close to $-K$. And $\varrho \approx 0$ in case that the tag is on level two. Specifically, we can distinguish different levels according to the following hard-decision metrics,

- **Level 1**: $\varrho \to K \Rightarrow \varrho > \frac{K}{2}$
- **Level 2**: $\varrho \to 0 \Rightarrow |\varrho| \leqslant \frac{K}{2}$,
- **Level 3**: $\varrho \to -K \Rightarrow \varrho < -\frac{K}{2}$.

Fig. 11 summarizes the proposed algorithm and the detailed procedure. The RSSI and phases are collected from the two tilted COTS RFID antennas. The measured phases are utilized to identify the order of tags along the trajectory based on the algorithm presented in Section III-B, namely lateral identification. Then the neighborhood of the RSSI profiles when the two tilted antennas are in front of the tag, which are calculated based on the lateral positioning results. The neighborhoods of the two RSSI profiles are divided into K equal segments. Through the comparison of the average RSSI in corresponding segments based on (9), we can distinguish different levels easily.

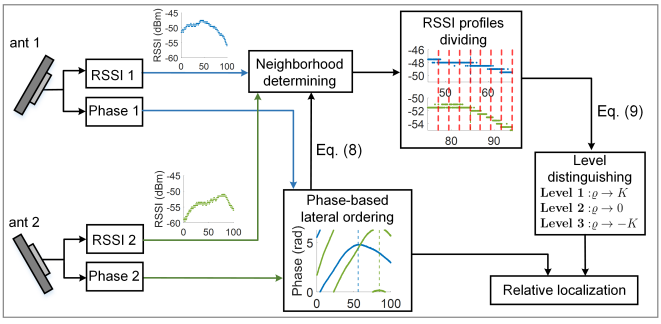

Fig. 11. Hybrid RSSI and phase relative positioning algorithm.

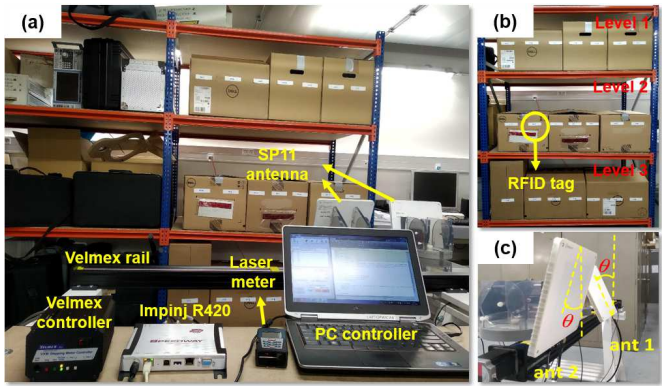

Fig. 12. The setups of the RFID relative positioning system (ReLoc): (a) the measurement campaign, (b) one case of the deployment of RFID tags, (c) the deployment of RFID antennas.

IV. Experiment and Results

A. Configuration

Based on the proposed relative localization algorithm, we implement a RFID ordering system (ReLoc). We adopt a COTS RFID reader Impinj Speedway R420 without any hardware modification, which works at the UHF band 865-868 MHz. Furthermore, two UHF RFID antennas (Keonn Advantenna-SP11), a PC controller and passive commercial tags (Alien G) are used. The RFID reader is connected to laptop controller that collects the low level user data (LLUD), through the Ethernet cable. The LLUD are recorded by the software on the laptop controller under the low level reader protocol (LLRP). Meanwhile, a Velmex positioning system is utilized and acts as the platform to move the antennas with mm-level accuracy. The Velmex controller connects with the PC controller via serial port.

The experiment is conducted in a virtual warehouse (i.e. lab environment with steel racks mimicking a warehouse), as shown in Fig. 12, which is a typical three-layers steel rack. On the metallic rack, 21 Alien G RFID tags with arbitrary orientations (X-axis tag rotation) are attached on the paper cartons. The size of the rack is $1.2m \times 2.2m$. The distance between each two levels is about 0.66 meters. Two antennas are deployed horizontally almost at the same height (0.91 meters) as the second level of the rack. The space (side to side) between two antennas is 10 centimeters. The distance from the antennas to the rack is 1.2 meters. In the experiment, we place the different items consisting of different materials into the paper cartons, namely glass, plastic and metal. We have repeated the experiments 20 times and collected the measured RSSI and phases, so there are 20×2 (antennas)$\times 21$ (tags)$= 840$ sets of RSSI or phases in total.

B. Parameters Discussion

In this section, we clarify the selection of the involved parameters aiming for the real-world deployment in a warehouse, namely the sloping angle θ, the judgment threshold γ, and the neighborhood length 2ϵ. The number of segments K will be discussed in Section IV-C.

1) Tilted Angle θ: As discussed above, when the antenna rotates along the Y-axis by 45 degrees (upwards or downwards), it will bring about 3.5$\sim$6 dB RSSI shifts. It should be noted that rotating the antenna by a larger angle will have more distinct RSSI shifts, which is better for level discrimination. But according to our experiment, it will also cause many records lost, especially when the incidence angle is larger than 60 degrees. In our RFID positioning prototype, the distance from the antenna to the rack is 1.2 meters and the distance between adjacent levels is around 0.66 meters. So the incidence angle is $\delta = \frac{180}{\pi}\arctan(\frac{0.66}{1.2}) \approx 28.8$ degrees for the level one or level three. If we rotate the antenna upwards by e.g., 20 degrees, for instance, the new incidence angle δ' will be 48.8 degrees for the level three, which satisfies the rotation requirement (45 degrees). Obviously, the tilted angle selection is determined by the distance from the antenna to the rack and the adjacent distance between the rack's level. Generally, each layer of the rack is almost equidistant in warehouse. Even if the adjacent distances between the layers have some deviations, they will not affect the performance due to the coarse-grained RSSI for level distinguishing. So in real-world applications, we can easily deploy the RFID positioning system after checking the racks in the warehouse.

2) Judgment Threshold γ: After setting the distance from the antenna to the rack and the tilted angle θ for two tilted antennas, we will have 3.5$\sim$6 dB offsets between the two antennas on the basis of the beamwidth of the selected antenna (Keonn Advantenna-SP11 in this paper). But actually, according to our observations, the received RSSI from the COTS reader (Impinj R420) have ± 0.5 dB jumps due to the hardware settings, even though the distance to the tag does not change. Thus the offsets may decrease to 3$\sim$5.5 dB. Furthermore, we set an additional margin of 0.5$\sim$1 dB smaller when considering the system noise and other interference. Thus, the threshold $\gamma = 2$ dB in the experiments.

3) Neighborhood Length 2ϵ: The neighborhood length 2ϵ of the RSSI profile decides how many samples will be used for the comparison. In the RFID positioning system, we use the neighborhood when the antenna is in front of the tag due to less lateral polarization mismatch. Since the RSSI is a coarse-grained metric and easily affected by the channel fading and polarization mismatch, we utilize the phase-based method to estimate the peak index ℓ_0 when the antenna is closest to the tag. However, the estimation of the peak index may have some errors (less than half wavelength according

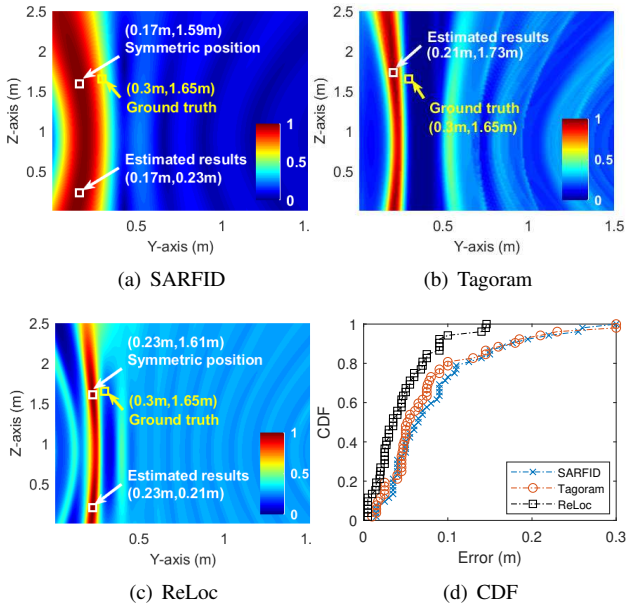

(a) SARFID (b) Tagoram

(c) ReLoc (d) CDF

Fig. 13. The lateral positioning performance.

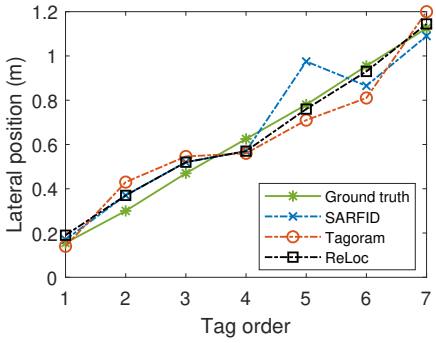

Fig. 14. One example of the estimated tag order.

to our experimental results). So we can set neighborhood length as the two times of maximum lateral estimation errors. In practical applications, we recommend to set 2ϵ to the wavelength (about 34.5 centimeters in the experiment).

4) Note to Practitioners: The proposed method is based on the COTS devices, so the characteristic of the hardware and the positioning scenario should be checked before the practical deployment in warehouses. Specifically, when in a new deployment, the practitioners should check the beamwidth of the selected antenna firstly. Take Keonn Advantenna-SP11 RFID antenna in this paper as an example, it is a circular-polarization antenna with 70-degree beamwidth. If the incidence angle from the antenna to the tag is larger than half beamwidth, it should observe more than 3 dB RSSI decrements than the antenna spindle, as shown in Fig. 3(c)-(d). To have a more distinct RSSI difference, we recommend the incidence angle δ' to be 15$\sim$20 degrees larger than half the beamwidth. Next, we can determine the tilted angle θ based on the description in Section IV-B.1. For the judgment threshold γ, it is related with the RSSI differences between the two tilted antennas. In the implementation, we recommend to set 0.5$\sim$1 dB additional margin smaller on the basis of the RSSI differences, due to the impact of hardware noise and other interference.

C. Results and Evaluation

1) Lateral Ordering: For lateral ordering, we use the phase-based variant MLE to estimate the lateral positions of RFID tags as presented in Section III-B. To mitigate the impact caused by phase shift φ_0 (including the shifts caused by the tag orientation), a differential augmentation scheme has been introduced. In the experiments, the first measured phase is chosen as the reference ($\phi_m[r]$ in (5)). To evaluate the lateral positioning accuracy, we present the positioning results based on the normalized hologram at the plane of the steel rack (namely, Y-axis and Z-axis). The normalized hologram illustrates the likelihood of tag position at the scale of the rack, which pinpoints the estimated result of the highest probability. We compare our method ReLoc with two state-of-art absolute positioning methods, namely SARFID [11] and Tagoram [10]. SARFID and Tagoram are both hologram-based algorithms under the framework of the SAR method. It should be noted that we deploy two antennas at the same altitude in our RFID positioning system. So there is a symmetric position ambiguity problem on the two sides of the antennas' trajectory. Figs. 13(a)-(c) show the estimated results of tag ♯2 on level one in Fig. 12. As shown in Figs. 13(a)(c), SARFID and ReLoc obtain the estimated positions close to the symmetric points of the ground truth about the trajectory. If we know the tag is above or below the trajectory, we also can obtain the absolute estimated positions. For instance, the symmetric Z-coordinate of the estimated result of ReLoc can be calculated as $0.91 \times 2 - 0.21 = 1.61$ meters, which is quite close to ground truth (1.65 meters).

But we use phase-based method for lateral ordering in this paper, so only lateral results are considered and compared among these methods here. In Fig. 13, compared with SARFID and Tagoram, ReLoc mitigates more deceptive positions with the relatively high likelihood, namely it has narrower candidate regions (in Fig. 13(c)). ReLoc achieves 0.07-meter lateral offsets towards the ground truth, which realizes lateral positioning with smaller errors compared to SARFID (0.13 meters) and Tagoram (0.09 meters). Fig. 13(d) presents cumulative distribution function (CDF) of ReLoc, SARFID, and Tagoram. We can see that ReLoc realizes finer-grained lateral resolution with higher accuracy (less than 0.15 meters). Further, Tagoram (0.1-meter errors with 80%) is slightly better than SARFID (0.13-meter errors with 80%) in the experiment due to the weighted augmentation in Tagoram.

We evaluate the ordering accuracy according to the metric that a tag is ordered correctly if and only if the detected order is exactly equal to the actual order of the tag. The metric function of ordering accuracy is given by [18], [20]

$$Accuracy = \frac{\#\ of\ tags\ ordered\ correctly}{\#\ of\ tags\ in\ total}. \qquad (10)$$

For example, Fig. 14 shows one case of the estimated results of seven tags on the rack. The correct order of these tags is $1-2-3-4-5-6-7$. SARFID estimates the tags with the order $1-2-3-4-6-5-7$, because the estimated position of tag ♯5 is larger than tag ♯6, even through the estimated errors of

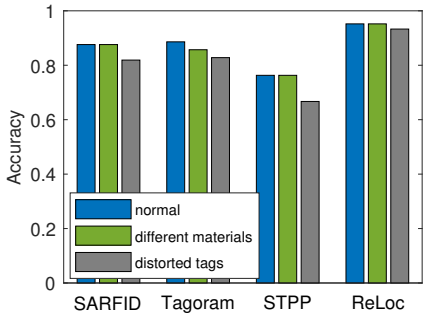

Fig. 15. Comparison of the lateral ordering accuracy.

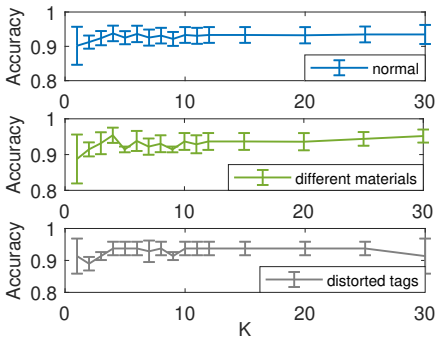

Fig. 16. K selection for level ordering.

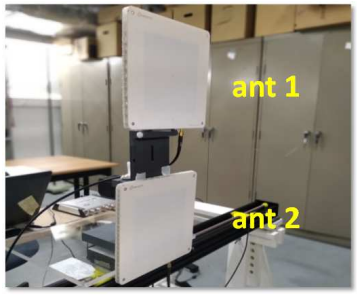

Fig. 17. Two vertical antennas deployment for SARFID and Tagoram.

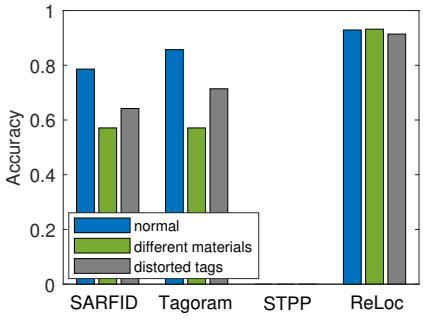

Fig. 18. Comparison of the level ordering accuracy.

tag ♯6 is as small as nine centimeters. Therefore, the ordering accuracy of SARFID in this example is $5/7 \doteq 71.4\%$. Both Tagoram and ReLoc achieve perfect order. However, Tagoram estimates the position of tag ♯3 (0.546 cm) and ♯4 (0.56 cm) with small differences. This means that the robustness of Tagoram is worse than ReLoc. Further, we evaluate the lateral distinguishing performance within three cases: normal, different materials, and distorted tags. '**Normal**' means that RFID tags are not distorted, and no metal/liquid objects inside the paper cartons. '**Different materials**' is the case that we place some items with different material, including four iron objects, one tank of water, etc. '**Distorted tags**' means the most of the tags are bent or folded as shown in Fig. 5(a). The average lateral ordering performance of ReLoc is presented, and compared with SARFID, Tagoram, and STPP in Fig. 15. Among them, STPP orders the tags through comparing the V-zone of their phase profiles [18], which gives the relative order directly. According to the experimental results in Table I, the proposed ReLoc outperforms the other methods in the three cases with average lateral ordering accuracy 94.6%, while the other methods obtain accuracy less than 88.6%. The results also indicate that distorted tags can decrease the ordering accuracy distinctly due to the possible records loss, especially for STPP. Further, different materials have nearly no effect on lateral ordering in our cases, which is because different materials inside the cartons have only a slight impact on the peak index distinguishing, as reported in Fig. 4, when the antennas are right in front of the tag.

2) Level Ordering: To distinguish different levels of RFID tags, we compare the RSSI profiles when the antennas are in front of the tag. The neighborhood $\mathbb{U}_\epsilon$ is divided into K segments for mean RSSI comparison. Fig. 16 shows that the level ordering accuracy with standard deviations (STDev) in three cases when we select different K values from one to 30. The results illustrate that the K selection slightly affects the average level ordering accuracy. But when the $K = 1$, the ordering accuracy presents the largest STDev (about 7%) compared with the cases that $K \geq 2$, which brings distinct uncertainty. Meanwhile, if the K is too large, there may be not enough RSSI records in the selected neighborhood $\mathbb{U}_\epsilon$, such as the fast-speed RFID positioning platform. So there is a note for the practitioners that it would be better to select K between two and 15 due to less fluctuation and computation. In this paper, we set $K = 4$.

Furthermore, we deploy the antennas at the same altitude in the experiments, so SARFID and Tagoram can not distinguish level one and level three due to the symmetric positions ambiguity. To compare the performance of algorithms fairly, we implement the two antennas vertically for SARFID's and Tagoram's validation without any other change of the other measurement setting. The distance between two antennas is also 10 centimeters, as shown in Fig. 17. On the other hand, STPP orders the tags of different levels through comparing their measured phases. But this method can not take effect when the distance difference Δd from two levels to the antenna is larger than a quarter wavelength (about 8.65 centimeters) as a result of phase ambiguity [18]. The distance difference between two adjacent levels in our experiment (namely $\sqrt{1.2^2 + 0.66^2} - 1.2 \approx 17$ centimeters) is too large for STPP to work. So in Table I and Fig. 18, we do not present the level results of STPP.

According to the experimental results, ReLoc performs much better than SARFID and Tagoram for level ordering. And ReLoc achieves 94.3% average accuracy for all these

TABLE I
LATERAL AND LEVEL ORDERING ACCURACY IN PERCENTAGE (%)

	Normal		**Different materials**		**Distorted tags**	
	lateral	level	lateral	level	lateral	level
SARFID [11]	87.6	78.6	87.6	57.1	81.9	64.2
Tagoram [10]	88.6	85.7	85.7	57.1	82.8	71.4
STPP [18]	76.3	/	76.3	/	66.7	/
ReLoc	**95.2**	**93.8**	**95.2**	**95.4**	**93.3**	**93.7**

TABLE II
COMPARISON OF THE AVAILABLE RFID LOCALIZATION METHODS

	SARFID [11]	**Tagoram** [10]	**STPP** [18]	**ReLoc** (this method)
Deployment	two vertical antennas	two vertical antennas	one antenna	two horizontal tilted antennas
System setting	coordinate system	coordinate system	/	tilted angle & distance
Materials contained or tag distortion	×	×	×	√
Not fully occupied racks	√	√	×	√
Anti-multipath	/	+	+	++
Average accuracy	lateral: 85.7%, level: 66.6%	lateral: 85.7%, level: 71.4%	lateral: 73.1%, level: /	lateral: 94.6%, level: 94.3%

three cases. Specifically, in case of '**normal**', SARFID does not obtain satisfying performance with 78.6% accuracy. This may be because of the multipath propagation in the positioning scenario (cluttered indoor deployment and steel rack). Tagoram achieves better results with 85.7% due to the weighted augmentation based on the CDF of the measured phases. ReLoc has the highest average accuracy with 93.8% for level ordering, and is immune to multipath effects because the two antennas will experience a very similar multipath environment. We only compare the RSSI profiles when the antennas are in front of the tags, so they experience almost the same fading. This means that the RSSI differences will only result from the antennas' rotation. Likewise, while different materials and distorted tags severely degrade the performance of SARFID and Tagoram, ReLoc still achieves a very high ordering accuracy (95.4%, and 93.7%, respectively), which shows the self-consistency and completeness of the proposed positioning system.

3) Analysis and Evaluation: Table II compares the system deployment and positioning performance of the proposed method (ReLoc) with the other three available state-of-the-art methods (SARFID, Tagoram, and STPP). Since we mainly consider the moving RFID positioning platform (such as drone-based system) for automatic warehouse management, the complexity of the whole system should be considered. In this paper, all the methods for comparison are based on COTS devices. SARFID, Tagoram, and ReLoc utilize two commercial antennas. STPP only adopt one antenna, but the robustness to the realistic applications and positioning performance are not satisfied in Table II.

SARFID and Tagoram are absolute-position based algorithms, which establish the Cartesian coordinate system to pinpoint the tags' coordinates. For the proposed ReLoc, it adopts two horizontal tilted antennas. It needs to set the tilted angle and distance from the antenna the rack as presented in Section IV-B, which is easy-deployment and feasible after checking the specific positioning scenario. For the different materials contained inside the cartons or parcels, and tag distortion, ReLoc outperforms the other methods since we distinguish the level order based on the RSSI differences of the two tilted antennas, which is immune to the materials contained in cartons and tag distortion. SARFID, Tagoram and ReLoc can work in case of not fully occupied racks, while STPP fails due to there is no reference for the phase profiles comparison.

SARFID and Tagoram localize the RFID tags based on the precise measured phase. But the multipath effect affects their performance severely. Tagoram performs better since all the input phases are weighted based on the CDF of measured phases. It augments the measured phases with less deviations, which achieves satisfied performance in low-multipath scenarios. STPP utilizes the warping and fitting phases to order the tags, but the effect of anti-multipath is limited. For the proposed ReLoc, it improves the lateral resolution with narrower candidate regions. Furthermore, ReLoc discriminates the level only based on the RSSI differences when the two tilted antennas are at the same position, such that the two antennas experience almost the same channel fading. So we conclude that ReLoc is more robust to multipath effect. Due to the advantages in these cases (in Table II), ReLoc achieves the best lateral and level ordering accuracy.

V. CONCLUSION

In this paper, we present a comprehensive analysis of the challenges for passive RFID positioning applications. For industrial inventory management in warehouses, RFID tag selection, orientation of the tag and antenna, material inside the carton, tag distortion, and multipath propagation affect the performance of RFID localization, as well as practical deployments. For this reason, we propose a relative localization method based on hybrid measured RSSI and phases.

- A variant maximum likelihood positioning method (the *sine* transformation) has been proposed to estimate the lateral positions of the tags, which results in an improved algorithm of the hologram-based solution with less than 15-centimeters lateral errors.
- Through comparing the RSSI profiles of two tilted antennas, we distinguish different levels avoiding the impacts of different materials contained in the carton, tag distortion and multipath propagation.
- According to our experimental results, the proposed method (ReLoc) achieves 94.6% average lateral ordering accuracy and 94.3% level accuracy, which outperforms the available state-of-the-art methods.

Overall, ReLoc can be a potential solution for automated inventory management in industrial environments. For the

future work, a real-world drone-based or robot-based ReLoc RFID positioning experiment will be conducted in warehouses. Instead of two tilted antennas, RSSI-based beamforming method based on the designed patch antennas can be utilized to distinguish the tags vertically. Furthermore, RFID relative localization can be regarded as a multi-class classification problem, so the RFID relative positioning based on machine learning can be a potential direction of the future work.

REFERENCES

[1] J. Tiemann and C. Wietfeld, "Scalable and Precise Multi-UAV Indoor Navigation using TDOA-based UWB Localization," in *2017 International Conference on Indoor Positioning and Indoor Navigation (IPIN)*, Sep 2017, pp. 1–7.

[2] DroneScan, "Physical Inventory - Stock Take, Physical Inventory, Cycle Counting (2018)," [Online]. Available: https://dronescan.co/info.

[3] E. Digiampaolo and F. Martinelli, "A Robotic System for Localization of Passive UHF-RFID Tagged Objects on Shelves," *IEEE Sensors Journal*, vol. 18, no. 20, pp. 8558–8568, Oct 2018.

[4] A. Buffi, A. Motroni, P. Nepa, B. Tellini, and R. Cioni, "A SAR-Based Measurement Method for Passive-Tag Positioning With a Flying UHF-RFID Reader," *IEEE Transactions on Instrumentation and Measurement*, vol. 68, no. 3, pp. 845–853, Mar 2019.

[5] InWareDrones, "Indoor Inventory DRONE Solution," [Online]. Available: https://www.imec-int.com/en/what-we-offer/research-portfolio/inwaredrones.

[6] L. M. Ni, Yunhao Liu, Yiu Cho Lau, and A. P. Patil, "LANDMARC: indoor location sensing using active RFID," in *Proceedings of the First IEEE International Conference on Pervasive Computing and Communications, 2003. (PerCom 2003).*, Mar 2003, pp. 407–415.

[7] J. Zhang, Y. Lyu, J. Patton, S. C. G. Periaswamy, and T. Roppel, "Bfvp: A probabilistic uhf rfid tag localization algorithm using bayesian filter and a variable power rfid model," *IEEE Transactions on Industrial Electronics*, vol. 65, no. 10, pp. 8250–8259, Oct 2018.

[8] P. V. Nikitin, R. Martinez, S. Ramamurthy, H. Leland, G. Spiess, and K. V. Rao, "Phase based spatial identification of UHF RFID tags," in *IEEE International Conference on RFID*, May 2010, pp. 102–109.

[9] R. Miesen, F. Kirsch, and M. Vossiek, "UHF RFID localization based on synthetic apertures," *IEEE Transactions on Automation Science and Engineering*, vol. 10, no. 3, pp. 807–815, Jul 2013.

[10] L. Yang, Y. Chen, X.-Y. Li, C. Xiao, M. Li, and Y. Liu, "Tagoram: Real-time Tracking of Mobile RFID Tags to High Precision Using COTS Devices," in *Proceedings of the 20th Annual International Conference on Mobile Computing and Networking*, ser. MobiCom '14, Sep 2014, pp. 237–248.

[11] A. Buffi, P. Nepa, and F. Lombardini, "A phase-based technique for localization of UHF-RFID tags moving on a conveyor belt: Performance analysis and test-case measurements," *IEEE Sensors Journal*, vol. 15, no. 1, pp. 387–396, Jan 2015.

[12] T. Liu, L. Yang, Q. Lin, Y. Guo, and Y. Liu, "Anchor-free Backscatter Positioning for RFID Tags with High Accuracy," in *IEEE Conference on Computer Communications*, Apr 2014, pp. 379–387.

[13] H. Ma, Y. Wang, K. Wang, and Z. Ma, "The Optimization for Hyperbolic Positioning of UHF Passive RFID Tags," *IEEE Transactions on Automation Science and Engineering*, vol. 14, no. 4, pp. 1590–1600, Oct 2017.

[14] Y. Ma, B. Wang, S. Pei, Y. Zhang, S. Zhang, and J. Yu, "An Indoor Localization Method Based on AOA and PDOA Using Virtual Stations in Multipath and NLOS Environments for Passive UHF RFID," *IEEE Access*, vol. 6, pp. 31 772–31 782, May 2018.

[15] Y. Ma, B. Wang, X. Gao, and W. Ning, "The Gray Analysis and Machine Learning for Device-Free Multi-target Localization in Passive UHF RFID Environments," *IEEE Transactions on Industrial Informatics*, pp. 1–1, 2019.

[16] H. Xu, D. Wang, R. Zhao, and Q. Zhang, "FaHo: Deep Learning Enhanced Holographic Localization for RFID Tags," in *Proceedings of the 17th Conference on Embedded Networked Sensor Systems*, ser. SenSys '19, Nov 2019, pp. 351–363.

[17] L. Shangguan, Z. Li, Z. Yang, M. Li, and Y. Liu, "OTrack: Order tracking for luggage in mobile RFID systems," in *2013 Proceedings IEEE INFOCOM*, Apr 2013, pp. 3066–3074.

[18] L. Shangguan, Z. Yang, A. X. Liu, Z. Zhou, and Y. Liu, "STPP: Spatial-Temporal Phase Profiling-Based Method for Relative RFID Tag Localization," *IEEE/ACM Transactions on Networking*, vol. 25, no. 1, pp. 596–609, Feb 2017.

[19] L. Shangguan and K. Jamieson, "The design and implementation of a mobile rfid tag sorting robot," in *Proceedings of the 14th Annual International Conference on Mobile Systems, Applications, and Services*, ser. MobiSys '16, Jun 2016, pp. 31–42.

[20] G. WANG, C. Qian, L. Shangguan, H. Ding, J. Han, K. Cui, W. Xi, and J. Zhao, "HMO: Ordering RFID Tags with Static Devices in Mobile Environments," *IEEE Transactions on Mobile Computing*, pp. 1–1, 2019.

[21] C. Li, E. Tanghe, D. Plets, P. Suanet, J. Hoebeke, E. De Poorter, and W. Joseph, "RePos: Relative Position Estimation of UHF-RFID Tags for Item-level Localization," in *IEEE International Conference on RFID Technology and Applications (RFID-TA)*, Sep 2019, pp. 357–361.

[22] T. Wei and X. Zhang, "Gyro in the Air: Tracking 3D Orientation of Batteryless Internet-of-things," in *Proceedings of the 22Nd Annual International Conference on Mobile Computing and Networking*, ser. MobiCom '16, Oct 2016, pp. 55–68.

[23] E. Tanghe, W. Joseph, L. Verloock, L. Martens, H. Capoen, K. V. Herwegen, and W. Vantomme, "The industrial indoor channel: large-scale and temporal fading at 900, 2400, and 5200 MHz," *IEEE Transactions on Wireless Communications*, vol. 7, no. 7, pp. 2740–2751, Jul 2008.

[24] J. Wang and D. Katabi, "Dude, Where's My Card?: RFID Positioning That Works with Multipath and Non-line of Sight," *SIGCOMM Comput. Commun. Rev.*, vol. 43, no. 4, pp. 51–62, Aug. 2013.

[25] Impinj, "Speedway revolution reader application note - low level user data support (revision 3.0, 2013)," [Online]. Available: https://support.impinj.com/hc/en-us/articleattachments/200774268/SR_AN_IPJ_Speedway_Rev_Low_Level_Data_Support_20130911.pdf.

[26] C. Li, E. Tanghe, D. Plets, P. Suanet, N. Podevijn, J. Hoebeke, E. De Poorter, L. Martens, and W. Joseph, "Phase-based Variant Maximum Likelihood Positioning for Passive UHF-RFID Tags," in *14th European Conference on Antennas and Propagation, EuCAP 2020*, Mar 2020, pp. 1–5.

[27] EPC Radio-Frequency Identity Protocols Generation-2 UHF RFID, "Specification for rfid air interface protocol for communications at 860 MHz – 960 MHz," [Online]. Available: https://www.gs1.org/sites/default/files/docs/epc/gs1-epc-gen2v2-uhf-airinterface_i21_r_2018-09-04.pdf, 2018.

[28] J. D. Griffin and G. D. Durgin, "Complete Link Budgets for Backscatter-Radio and RFID Systems," *IEEE Antennas and Propagation Magazine*, vol. 51, no. 2, pp. 11–25, April 2009.

[29] J. S. Choi, M. Kang, R. Elmasri, and D. W. Engels, "Investigation of impact factors for various performances of passive uhf rfid system," in *2011 IEEE International Conference on RFID-Technologies and Applications*, Sep 2011, pp. 152–159.

[30] C. Jiang, Y. He, X. Zheng, and Y. Liu, "Orientation-aware rfid tracking with centimeter-level accuracy," in *2018 17th ACM/IEEE International Conference on Information Processing in Sensor Networks (IPSN)*, Apr 2018, pp. 290–301.

[31] J. Wang, L. Chang, O. Abari, and S. Keshav, "Are RFID Sensing Systems Ready for the Real World?" in *Proceedings of the 17th Annual International Conference on Mobile Systems, Applications, and Services*, ser. MobiSys '19, Jun 2019, pp. 366–377.

[32] J. Wang, J. Xiong, H. Jiang, X. Chen, and D. Fang, "D-Watch: Embracing Bad Multipaths for Device-Free Localization With COTS RFID Devices," *IEEE/ACM Trans. Netw.*, vol. 25, no. 6, pp. 3559–3572, Dec. 2017.

[33] Z. Wang, M. Xu, N. Ye, R. Wang, and H. Huang, "RF-Focus: Computer Vision-assisted Region-of-interest RFID Tag Recognition and Localization in Multipath-prevalent Environments," *Proc. ACM Interact. Mob. Wearable Ubiquitous Technol.*, vol. 3, no. 1, pp. 29:1–29:30, Mar. 2019.

[34] R. Zhao, Q. Zhang, D. Li, H. Chen, and D. Wang, "A novel accurate synthetic aperture rfid localization method with high radial accuracy," in *2017 IEEE 18th International Symposium on A World of Wireless, Mobile and Multimedia Networks (WoWMoM)*, Jun 2017, pp. 1–9.